



Limitations of Lattice Boltzmann Modeling of Micro-Flows in Complex Nanopores

ZUO Hong^{1,2}, DENG Shouchun^{1,*} and LI Haibo¹

¹ State Key Laboratory of Geomechanics and Geotechnical Engineering, Institute of Rock and Soil Mechanics, Chinese Academy of Sciences, Wuhan 430071, China.

² University of Chinese Academy of Sciences, Beijing 100094, China

Abstract: The multiscale transport mechanism of methane in unconventional reservoirs is dominated by slip and transition flows resulting from the ultra-low permeability of micro/nano-scale pores, which requires consideration of the microscale and rarefaction effects. Traditional continuum-based computational fluid dynamics (CFD) becomes problematic when modeling micro-gaseous flow in these multiscale pore networks because of its disadvantages in the treatment of cases with a complicated boundary. As an alternative, the lattice Boltzmann method (LBM), a special discrete form of the Boltzmann equation, has been widely applied to model the multi-scale and multi-mechanism flows in unconventional reservoirs, considering its mesoscopic nature and advantages in simulating gas flows in complex porous media. Consequently, numerous LBM models and slip boundary schemes have been proposed and reported in the literature. This study investigates the predominately reported LBM models and kinetic boundary schemes. The results of these LBM models systematically compare to existing experimental results, analytical solutions of Navier-Stokes, solutions of the Boltzmann equation, direct simulation of Monte Carlo (DSMC) and information-preservation DSMC (IP_DSMC) results, as well as the numerical results of the linearized Boltzmann equation by the discrete velocity method (DVM). The results point out the challenges and limitations of existing multiple-relaxation-times LBM models in predicting micro-gaseous flow in unconventional reservoirs.

Key words: LBM, DVM, micro-gaseous flow, slip boundary schemes, effective viscosity, flow regimes

Citation: Zuo et al., 2019. Limitations of Lattice Boltzmann Modeling of Micro-Flows in Complex Nanopores. Acta Geologica Sinica (English Edition), 93(6): 1808–1822. DOI: 10.1111/1755-6724.14289

1 Introduction

The micro-flows with large Knudsen-numbers are frequently encountered in emerging high-tech industries, environments, and traditional energy fields, e.g., micro-electromechanical systems (MEMS), nano-electromechanical systems (NEMS), microfluidic technology and microfluidic devices (Chen and Hu, 2015), and environments and the exploitation of unconventional reservoirs (Wang and Sheng, 2017; Liu, Huihai et al., 2018). The Knudsen number Kn is defined as the ratio of the mean free path of gas molecule γ to the pores size D or local characteristic length H , namely, $Kn = \gamma/H$. For gas flows in irregular pores/channels, the Knudsen number is a local geometry-dependent parameter influenced by various factors, such as temperature, gas pressure, local characteristic length of pores/channels, etc. In the case when the pore sizes are of the same magnitude as the mean free path of gas molecules, a variety of abnormal phenomena occur as fluid flows into these micro/nanoscale pores. These phenomena include the velocity slip at walls, temperature jump near the walls, the Knudsen paradox, thermal transpiration, velocity inversion in micro cylindrical Couette flow, etc. (Su et al., 2017; Liu

et al., 2018). Additionally, a recent study (Wang et al., 2016) showed that micro-flows in micro/nano-pores are likewise influenced by fluid properties and solid surface. The authors' comparative studies (Wang et al., 2016) on the methane transport in graphene, quartz, and calcite nanopores indicate that the flow behavior of methane is affected by the strong attractive potential due to the presence of solid materials, thereby resulting in the attachment of methane gas to the solid surface and the formation of adsorbed layers. In this case, the methane flow into the nano/micro-pores is controlled by the coupling of micro-flows and adsorption/desorption effects (Zuo et al., 2019). Thus, accurate understanding and capturing of these phenomena induced by the microscale flow and the rarefaction effect are essential to guide the practice and operation of high-technology, as well as the productivity prediction of unconventional reservoirs. As the local characteristic length of pores decreases, the Knudsen number might increase to reach a critical value where the continuum-based models break down, e.g. $Kn = 0.1$. In this case, the continuum-based Navier-Stokes equations are not valid, and the micro-gaseous flow can be described by the Boltzmann equation (BE) (Chapman and Cowling, 1953), which can cover all flow regimes ranging from the continuum flow regime to the free molecule flow regime (Verhaeghe et al., 2009). The Boltzmann equation

* Corresponding author. E-mail: scdeng@whrsm.ac.cn

is extremely complicated, and it was simplified to the well-known Bhatnagar-Gross-Krook (BGK) model by introducing a simple collision model with a single relaxation time.

Extensive studies and numerical algorithms have been conducted to solve gas flow, including molecular dynamics simulations (MD) (Xue et al., 2015; Liu et al., 2015; Zhao et al., 2016b; Lin et al., 2017; Yu et al., 2017), direct simulation of Monte Carlo (DSMC) (Bird, 1994; Christou and Dadzie, 2016; Geng et al., 2016), the lattice Boltzmann method (LBM) (Shan et al., 2006; Qian et al., 2007; Qiao et al., 2013; Ning et al., 2014; Zhang et al., 2016; Cudjoe and Barati, 2017), discrete velocity method (DVM) (Su et al., 2017; Liu et al., 2018), and traditional computational fluid dynamics (CFD). The CFD model is not applicable to the cases where the continuum hypothesis breaks down, e.g. $Kn > 0.1$, while MD has difficulty in extending its applications to the macro-scale due to high computational costs. The other three numerical methods (DSMC, LBM, and DVM) can be regarded as numerical schemes for solving the Boltzmann equation. Despite achieving great success in modeling high-speed non-equilibrium flows, the DSMC has significantly limited its wider application to the low-speed rarefied flows due to statistical noise and high computational cost. Both LBM and DVM approximately solve the Boltzmann equation with a small number of discrete velocities (Su et al., 2017). In particular, the LBM can be regarded as a simplified version of DVM for the lesser but highly isotropic discrete velocities, which are employed to improve the computational efficiency. Applying the multi-scale analysis, the LBM can recover the Navier-Stokes equations at the low Mach number assumption (Guo and Shu, 2013). Thus, LBM can serve as an alternative to the numerical solvers of Navier-Stokes equations, thereby increasingly becoming a promising CFD solver in various fields. Additionally, a better understanding of the transport mechanism of micro-gaseous flow in nano/micro-scale porous media is critical to effectively guide the extraction of shale gas, as the pore sizes in shale reservoirs are extremely small with a wide range from 2 nm to 100 nm (Landry et al., 2016). The micro-gaseous flow in the complex pores is controlled by the slip and transition flows, which fall beyond the scope of some existing numerical methods, such as MD, DSMC, and traditional CFD. The modeling of high Knudsen-number flows in complex porous media via DVM is also a challenging task, as more discrete velocities are required to capture large discontinuities of the velocity distribution function (Su et al., 2017). To overcome the aforementioned issues, the LBM, with less but highly isotropic velocities, is widely chosen as a CFD solver for micro-gaseous flow in porous media (Wang et al., 2016; Zhao et al., 2016a; Zheng et al., 2017) due to its mesoscopic nature and advantages in addressing the complex boundary (including the non-slip boundary and slip boundary).

Over the last 30 years, some progress has been achieved in modeling the micro-gaseous flow with LBM, especially MRT-LBM (Guo et al., 2008; Chai et al., 2010; Tao and Guo, 2015). However, the MRT-LBM, as a continuum-

based CFD solver in nature, has a limited applicability to the transition flow, and free-molecule flow regimes for the Navier-Stokes equations are not valid in these flow regimes. Extensive studies by Guo et al. (Guo et al., 2007b; Guo and Zheng, 2008; Guo et al., 2008), Tang et al. (Tang et al., 2008), and Zhang et al. (Zhang et al., 2006) have extended the LBM model to simulate the micro-flows involving large Knudsen-number by introducing the kinetic boundary (e.g. the discrete Maxwellian boundary (DM) (Ansumali and Karlin, 2002), the combined diffusive reflection and bounce-back scheme (DBB) (Verhaeghe et al., 2009; Chai et al., 2010), and the combined bounce-back scheme and specular reflection (BSR) (Succi, 2002)) to address the velocity-slip at a wall, as well as the effective viscosity (Zhang et al., 2006; Guo et al., 2007b; Guo and Zheng, 2008; Guo et al., 2008; Tang et al., 2008) to correct the nonlinear constitutive equation induced by rarefaction effect. Nevertheless, their strategies that correct the effective viscosity to model the rarefied gas flows with a high Knudsen-number are mainly established according to a straight long-microchannel. Although these related studies can accurately predict the high Knudsen number gas flows in the long-channel (Guo et al., 2008), their LBM models are actually equivalent to the Navier-Stokes equations combined with the corrected constitutive equations and slip boundary schemes. Thus, whether these LBM models can provide good predictions for the complicated porous media needs further validation.

Several important and encouraging studies (Su et al., 2017; Wu et al., 2017; Liu et al., 2018) were designed to address this issue via DVM, or to accurately solve the linearized BGK equation. Su and Wu et al. (Su et al., 2017) solved the large Knudsen number flows in three porous media with DVM and compared to existing results predicted by Zhao et al. (Zhao et al., 2016a) with the multiple-relaxation-time LBM (MRT-LBM). Their comparisons demonstrate that the MRT-LBM model cannot accurately simulate rarefied gas flows in complicated porous media. However, only a few predicted results by MRT-LBM were available and were thus included in these comparisons. By directly solving the linearized BGK equation, Wu et al. (Wu et al., 2017) systematically studied rarefied gas flows in simplified porous media, pointing out some limitations of the Klinkenberg model and Navier-Stokes equations with the first-order velocity-slip boundary scheme. Recently, Liu et al. (Liu et al., 2018) modeled micro-gaseous flow in the bend micro-channels by solving the BGK equation with DVM. Their results indicate that the predicted flux is not only controlled by the rarefaction effect but also by the shape and bend angle of micro-channels. Therefore, to some extent, the direct applicability of these models derived from the simplest geometries (such as straight channel or tubes) to more complicated porous media may be inaccurate and hence problematic. Fortunately, in recent studies (Su et al., 2017; Wu et al., 2017) rarefied gas flows in some complex porous media were accurately modeled by directly solving the linearized BGK equation with DVM. These can be set as benchmark cases and enable us to model the rarefied gas flows in the same

porous media under the same conditions with MRT-LBM. In this study, we perform extensive studies on two popular kinetic boundary schemes of LBM (DBB and DM boundary scheme). The calculated results are compared to the existing experimental results, the analytical solutions of Navier-Stokes, solutions of Boltzmann equation, DSMC/IP_DSMC results, and the predicted results (Su et al., 2017; Wu et al., 2017) with DVM, revealing some limitations of the existing MRT-LBM while modeling high Knudsen number flow in complex porous media. We finally approximately obtain a critical Knudsen number below which the MRT-LBM combined with kinetic boundary scheme can provide reliable results.

Although micro-gaseous flows are affected by the pore sizes, fluid properties, and solid surface, etc. (Wang et al., 2016), in this study, we mainly put our emphasis on microscale and rarefaction effects induced by pore sizes, at the absence of adsorption/desorption effects. This paper is organized as follows. The second section introduces the MRT-LBM numerical method, several popular kinetic boundary schemes for microscale flow, the regularization procedure, the calculation of local characteristic length and local Knudsen number, and eventually the validation cases. The third section presents the LBM modeling of micro-gaseous flow in the porous media reported in the references (Su et al., 2017; Wu et al., 2017), and finally we conduct a systematic comparative study on the MRT-LBM and DVM. The fourth section draws conclusion according to our comparative studies and further outlines future directions.

2 Lattice Boltzmann Method and Boundary Condition

2.1 D2Q9 multi-relaxation-time (MRT) LBM model

The lattice Boltzmann method is a mesoscopic numerical method for computational fluid dynamics. Applying the multi-scale analysis developed by Chapman and Enskog, the Navier-Stokes equations can be recovered from the lattice Boltzmann equation. The expression of the lattice Boltzmann equation with external force can be arranged as follows

$$f_i(x + c_i \delta_i t + \delta_i) - f_i(x, t) = \mathcal{Q}(f_i) + \delta t F_i \quad (2.1)$$

where $f_i(x, t)$ is the particle distribution function, δ_i is the time increment, the term $\mathcal{Q}(f_i)$ on the right hand is the collision operator, and F_i is the external force in the i th direction defined by

$$F = \mathbf{M}^{-1}(\mathbf{I} - \mathbf{S}/2)\mathbf{M}\bar{F}, \quad \bar{F}_i = w_i \left[\frac{c_i \cdot \mathbf{G}}{c_s^2} + \frac{\mathbf{u}\mathbf{G} : (c_i c_i - c_s^2 \mathbf{I})}{c_s^4} \right] \quad (2.2)$$

where \mathbf{G} is the external force in physical model, \mathbf{M} is the orthogonal matrix, \mathbf{S} is the relaxation time matrix, w_i is the weight in the i th direction, and c_s is the sound speed of the lattice. The D2Q9 model with nine velocities is adopted in this study to model fluid flow through porous media. Its velocity directions are defined as:

$c_0=(0,0)$, $c_1=(1,0)$, $c_2=(-1,0)$, $c_3=(0,1)$, $c_4=(0,-1)$, $c_5=(1,1)$, $c_6=(-1,-1)$, $c_7=(1,-1)$, and $c_8=(-1,1)$.

The orthogonal matrix \mathbf{M} related to above velocity directions is expressed as

$$\mathbf{M} = \begin{bmatrix} 1 & 1 & 1 & 1 & 1 & 1 & 1 & 1 & 1 \\ -4 & -1 & -1 & -1 & -1 & 2 & 2 & 2 & 2 \\ 4 & -2 & -2 & -2 & -2 & 1 & 1 & 1 & 1 \\ 0 & 1 & -1 & 0 & 0 & 1 & -1 & 1 & -1 \\ 0 & -2 & 2 & 0 & 0 & 1 & -1 & 1 & -1 \\ 0 & 0 & 0 & 1 & -1 & 1 & -1 & -1 & 1 \\ 0 & 0 & 0 & -2 & 2 & 1 & -1 & -1 & 1 \\ 0 & 1 & 1 & -1 & -1 & 0 & 0 & 0 & 0 \\ 0 & 0 & 0 & 0 & 0 & 1 & 1 & -1 & -1 \end{bmatrix} \quad (2.3)$$

Generally, the collision operator $\mathcal{Q}(f_i)$ is a nonlinear integral differential expression in terms of the particle distribution function $f_i(x, t)$. The MRT model with the well-known linearized collision operator $\mathcal{Q}(f_i)$ is employed in this study, which can be expressed as (Tao and Guo, 2015)

$$\mathcal{Q}(f_i) = -(\mathbf{M}^{-1}\mathbf{S}\mathbf{M}) [f(x, t) - f^{(eq)}(x, t)] \quad (2.4)$$

where $f(x, t) = [f_0(x, t), f_1(x, t), \dots, f_8(x, t)]$, and $f^{(eq)}(x, t) = [f_0^{(eq)}(x, t), f_1^{(eq)}(x, t), \dots, f_8^{(eq)}(x, t)]$ is the vector of the equilibrium distribution functions.

The relaxation time matrix is given as follows

$$\mathbf{S} = \begin{bmatrix} \tau_\rho^{-1} & & & & & & & & \\ & \tau_e^{-1} & & & & & & & \\ & & \tau_\varepsilon^{-1} & & & & & & \\ & & & \tau_d^{-1} & & & & & \\ & & & & \tau_q^{-1} & & & & \\ & & & & & \tau_d^{-1} & & & \\ & & & & & & \tau_q^{-1} & & \\ & & & & & & & \tau_s^{-1} & \\ & & & & & & & & \tau_s^{-1} \end{bmatrix} \quad (2.5)$$

Where τ_s is the non-dimensional relaxation time, and other parameters can be found in Guo et al. (Guo and Shu, 2013). The relaxation time τ_s is related to the kinematic viscosity as

$$\nu = \frac{\mu}{\rho} = c_s^2 (\tau_s - 0.5) \delta_i \quad (2.6)$$

Their $f_i^{(eq)}(x, t)$ Equation is the equilibrium distribution function in the i th direction, which can be determined by the macroscopic Navier-Stokes equations and conservation forms of the moments (Guo and Shu, 2013). The above lattice Boltzmann Equation combined with Equation is referred to as the MRT-LBM model, in which $f_i^{(eq)}(x, t)$ can be given as

$$f_i^{(eq)}(x, t) = w_i \rho \left[1 + \frac{c_i \cdot \mathbf{u}}{c_s^2} + \frac{\mathbf{u}\mathbf{u} : (c_i c_i - c_s^2 \mathbf{I})}{2c_s^4} \right] \quad (2.7)$$

with \mathbf{u} and ρ denoting the velocity and density of the fluid, respectively.

The macroscopic quantities, e.g. density ρ , velocity \mathbf{u} and pressure p , can be expressed in terms of the distribution function $f_i(x, t)$ as follows

$$\begin{aligned}\rho &= \sum_{i=0}^8 f_i \\ \rho \mathbf{u} &= \sum_{i=0}^8 f_i \mathbf{c}_i + G / 2 \\ p &= \rho c_s^2\end{aligned}\quad (2.8)$$

where c_s is the lattice sound speed, which is equal $1/\sqrt{3}$ to in the D2Q9 model.

For microscale flow, the widely recognized dimensionless parameter is the Knudsen number. The relaxation time is further determined by the Knudsen number, as

$$\tau_s = 0.5 + Kn \cdot H \cdot \sqrt{\frac{6}{\pi}} \quad (2.9)$$

where Kn is the Knudsen number, and H is the characteristic length.

For the gaseous flow in confined pores at a moderate Knudsen number, the Knudsen layer should be properly addressed. The popular strategy is to correct the mean free path of the gas molecule or viscosity to solve the large Knudsen number flow in the framework of the Navier-Stokes equations derived under the continuum assumption. Guo et al. (Guo et al., 2006; Guo et al., 2007b) introduced the effective viscosity correction into the LBM to model micro-gaseous flow at a finite Knudsen number. Li et al. (Li et al., 2011) incorporated the well-known Bosanquet-type effective viscosity into LBM to capture micro-flows in slip and early transition flow regimes. The Bosanquet-type effective viscosity is the mean effective viscosity across the cross-section, and it is only dependent on the local Knudsen number. For the sake of simplicity, we adopt the following Bosanquet-type effective viscosity to capture the effects of the Knudsen layer

$$\mu_e = \frac{\mu}{1 + 2 \cdot Kn} \quad (2.10)$$

where μ and μ_e are the dynamic viscosity and effective dynamic viscosity of the fluid, respectively.

Taking Equations (2.6), (2.9), and (2.10) into consideration, we obtain the effective viscosity-related relaxation time τ_s as

$$\tau_s = 0.5 + Kn \cdot H \cdot \sqrt{\frac{6}{\pi}} \cdot \frac{1}{1 + 2 \cdot Kn} \quad (2.11)$$

2.2 Kinetic boundary schemes for velocity-slip

The pore sizes in shale range from 2 nm to 100 nm, and the Knudsen number in these micro/nanopores is generally larger than 0.001. Thus, the micro-gaseous flow in these microscale pores is affected by the microscale effect (e.g., the velocity slip at the solid surface) and the rarefaction effect. The slip velocity induced by the microscale effect can be determined by a first-order or second-order velocity-slip boundary condition. In the existing LBM models, two popular boundary schemes are widely employed to capture the velocity slip along the curved walls: the discrete Maxwellian boundary (DM), and the combined diffusive reflection and bounce-back scheme

(DBB).

The DM boundary scheme developed by Ansumali and Karlin (Ansumali and Karlin, 2002) can be regarded as a discrete form of the full diffuse reflection boundary scheme. The unknown particle distribution function at the boundary point, determined by this boundary scheme, is given as follows

$$\begin{aligned}f_i^{DM}(x, t) &= K f_i^{(eq)}(\rho_w, \mathbf{u}_w) \\ K &= \frac{\sum_{\xi_i \cdot \mathbf{n} < 0} |\xi_i \cdot \mathbf{n}| f_i'}{\sum_{\xi_i \cdot \mathbf{n} > 0} |\xi_i \cdot \mathbf{n}| f_i^{(eq)}(\rho_w, \mathbf{u}_w)}, \quad \xi_i' = \mathbf{c}_i - \mathbf{u}_w\end{aligned}\quad (2.12)$$

where \mathbf{n} is the normal vector at the wall, ρ_w is the density at the wall, \mathbf{u}_w is the velocity of wall, and f_i' is the post-collision distribution function determined by Equation (2.4) as $f_i' = f_i(x, t) + \Omega(f_i)$. For the discrete lattice, determining the normal direction of the wall is challenging. Therefore, the DM boundary scheme is generally implemented based on its physical concept, which assumes that the outgoing particles will reflect into the fluid, following the discrete Maxwellian law. For the static wall, Equation (2.12) can be further simplified to

$$f_i^{DM}(x, t) = \frac{w_i}{\sum_j w_j} \sum_j f_j' \quad (2.13)$$

where $\sum_j f_j'$ indicates the sum of post-collision particle distribution functions incident to the wall, while $\sum_j w_j$ is the total weight of outgoing particle distribution functions. The relaxation time matrix for the DM boundary scheme is chosen according to Zhao et al. (Zhao et al., 2016a)

$$S = \text{diag} \left(1.0, 1.19, 1.4, 1.0, \frac{8 \cdot (2 - 1/\tau_s)}{(8 - 1/\tau_s)}, 1.0, \frac{8 \cdot (2 - 1/\tau_s)}{(8 - 1/\tau_s)}, 1/\tau_s, 1/\tau_s \right) \quad (2.14)$$

where τ_s is the viscosity-related relaxation time determined by Equation .

The combined DBB, developed by Chai et al. (Chai et al., 2008) and Luo et al. (Verhaeghe et al., 2009), is adopted in this study to investigate the velocity slip at a random curved wall for its independence from the normal vector of wall. This can be expressed as

$$f_i = (1 - r) K f_i^{(eq)}(\rho_w, \mathbf{u}_w) + r f_i' \quad (2.15)$$

where \bar{i} indicates the opposite direction of i , r is the accommodated coefficient, the definitions of ρ_w and \mathbf{u}_w are the same with Equation (2.12). K is the normalization factor ensuring mass conservation, and can be expressed as

$$K = \frac{\sum_{\xi_i \cdot \mathbf{n} < 0} |\xi_i \cdot \mathbf{n}| f_i'}{\sum_{\xi_i \cdot \mathbf{n} > 0} |\xi_i \cdot \mathbf{n}| f_i^{(eq)}(\rho_w, \mathbf{u}_w)}, \quad \xi_i' = \mathbf{c}_i - \mathbf{u}_w \quad (2.16)$$

where f_i' is the post-collision distribution function, \mathbf{n} is the inward normal vector, and the definitions of remaining parameters are the same with Equation (2.12).

Considering Equation , for the static wall, the DBB boundary scheme (Equation) can be given as

$$f_i = (1-r) \cdot \sum_j \frac{w_j}{w_j} \sum_j f_j' + r f_i' \quad (2.17)$$

where $\sum_j f_j'$ indicates the sum of post-collision distribution functions streaming toward the solid node, and $\sum_j w_j$ is the sum of weights of corresponding distribution functions streaming toward the solid node.

To incorporate the velocity-slip boundary condition into the DBB boundary scheme, the accommodated coefficient r should be chosen as for the multi-relaxation-time model (Tao and Guo, 2015):

$$r = \frac{C_1(0.5 - \tau_s) + (\tau_s + \Delta - 1)\sqrt{6/\pi}}{C_1(\tau_s - 0.5) + (\tau_s - \Delta)\sqrt{6/\pi}} \quad (2.18)$$

where Δ equals to 0.5 in this study, C_1 is the coefficient of velocity-slip boundary scheme, and τ_1 is the viscosity-related relaxation time determined by Equation (2.11).

The relaxation time matrix for the DBB boundary scheme is chosen as according to Tao et al. (Tao and Guo, 2015)

$$\mathbf{S} = \text{diag}(1.0, 1.0/1.1, 1.0/1.2, 1.0, 1/\tau_q, 1.0, 1/\tau_q, 1/\tau_s, 1/\tau_s) \quad (2.19)$$

where the relaxation time related to τ_q is set as

$$\tau_q = \frac{C_2\pi}{4}(\tau_s - 0.5) + \frac{(6\Delta - 1)r\tau_s + (5 - 6\Delta)\tau_s + (0.5 - 3\Delta^2)r - 3\Delta^2 + 6\Delta - 2.5}{4(\tau_s - 0.5)(r + 1)} \quad (2.20)$$

with $C_1=1.1466$, $C_2=0.9757$ for the full diffuse wall (Guo and Shu, 2013).

Another kinetic boundary scheme gains popularity in the modeling micro-flows. This is the combined bounce-back scheme and specular reflection, which was firstly proposed by Succi (Succi, 2002) and later developed by Guo et al. (Guo et al., 2007a; Guo and Zheng, 2008) and Li et al. (Li et al., 2011). The BSR boundary scheme is restrained to some simple geometries (such as a straight channel), as it relies on the normal direction of wall. Thus, this boundary scheme is not included in this study due to its limited applicability to shale reservoirs.

To ensure that this MRT-LBM scheme is more accurate and stable in the hydrodynamic regime and beyond, a regularization step developed by the previous studies (Latt and Chopard, 2006; Zhang Raoyang et al., 2006; Suga, 2013) is adopted to model micro-gaseous flows with a high Knudsen number. In this regularization procedure, the distribution functions are decomposed into the equilibrium part and non-equilibrium part as (Suga, 2013)

$$f_i(x, t) = f_i^{(eq)}(x, t) + f_i^{(neq)}(x, t) \quad (2.21)$$

The non-equilibrium part $f_i^{(neq)}(x, t)$ can be converted to

$$\bar{f}_i^{(neq)}(x, t) = w_i \left[\frac{1}{2c_s^2} He_{mn}^{(2)} \left(\frac{c_i}{c_s} \right) \sum_{k=0}^8 f_k^{(neq)} c_{km} c_{kn} \right] \quad (2.22)$$

where $He_{mn}^{(2)}(\xi) = \xi_m \xi_n - \delta_{mn}$, $f_k^{(neq)}$ is the non-equilibrium distribution function defined as $f_i^{(neq)}(x, t) = f_i(x, t) - f_i^{(eq)}(x, t)$, where subscripts m and n are the dummy indices that obey Einstein's summation convention.

The evolution equation for the MRT-LBM model after the regularized procedure can be expressed as (Suga,

2013)

$$f(x + c_i \delta_t, t + \delta_t) = f^{(eq)}(x, t) + \bar{f}^{(neq)}(x, t) - (\mathbf{M}^{-1} \mathbf{S} \mathbf{M}) \bar{f}^{(neq)}(x, t) + \mathbf{M}^{-1} (\mathbf{I} - \mathbf{S} / 2) \mathbf{M} \bar{f} \quad (2.23)$$

2.3 Local characteristic length and local Knudsen number

For the micro-gaseous flow in complicated porous media, the Knudsen number is a local geometry-dependent parameter associated with space location due to the spatial variation of its influencing factors, such as temperature, gas pressure, local characteristic length, etc.

For the hard sphere molecule, the mean free path of gas molecules can be expressed as (Zhao et al., 2016a)

$$\lambda = \frac{m}{\sqrt{2}\pi\rho\sigma^2} \quad (2.24)$$

where m and ρ are the molecule mass and gas density, and σ is the molecule diameter.

With Equation (2.24), the Knudsen number for the ideal gas is given as

$$Kn_{loc} = \frac{\lambda}{H_{loc}} = \frac{m}{\sqrt{2}\pi\rho_{loc}\sigma^2 H_{loc}} = \frac{RT}{\sqrt{2}\pi P_{loc} N_A \sigma^2 H_{loc}} \quad (2.25)$$

where R and T are the gas constant and temperature, respectively, and N_A is the Avogadro constant. P_{loc} and H_{loc} are the local pressure of gas and local characteristic length of porous media, respectively (Zuo et al., 2019). Equation (2.25) is used to determine the local Knudsen number of a pore node in this study. To accurately capture the velocity slip along the surface, inspired by the studies by Zhao et al. (Zhao et al., 2016a; Zhao et al., 2016b), we propose the following concise method to determine the local characteristic length:

(1) The first step is to obtain the skeleton line of random porous media. A thinning algorithm for digital patterns proposed by Zhang (Zhang and Suen, 1984) is employed in this study. It consists of two subiterations with the aim of deleting boundary points to obtain the skeleton of unitary thickness for random patterns.

(2) After obtaining the skeleton of the pore space, the local characteristic length of a skeleton point is determined by the maximal ball algorithm (Silin and Patzek, 2006).

(3) The local characteristic length of a pore node equals to that of its nearest skeleton point according to its definition.

2.4 Validation: micro-gaseous flow in long channel

In this section, we first validate the cases with micro-gaseous flow in the periodic microchannel with a Knudsen number over a wide range. The validation model is set as follows: 1) the size of lattice is set as $N_x = 50$ and $N_y = 50$; 2) a constant pressure gradient $\partial p / \partial x = 10^{-4}$ in the

streamwise direction is applied to drive flow, and the inlet and outlet boundaries are the periodic boundary; 3) the slip boundary schemes (DM and DBB) introduced in Section 2.2 are exerted on the top and bottom walls. To validate the effectiveness of the DM and DBB boundary in

predicting micro-gaseous flow in a straight channel, we first calculate the non-dimensional mass flow rate as a function of the Knudsen number. The non-dimensional mass flow rate is defined as follows (Li et al., 2011)

$$Q = \frac{\int_0^H u_x dy}{(a_x H^2 \sqrt{RT/2/p})} \quad (2.26)$$

where $a_x = \partial p / \partial x = 10^{-4}$, is the channel width, is gas pressure, and the is determined by the sound speed of the lattice as $c_s = \sqrt{RT}$.

The present results are compared with the Boltzmann equation solution (Cercignani et al., 2004), Navier-Stokes solution with the second-order velocity-slip boundary scheme (Hadjiconstantinou, 2003), the MRT-LBM results with the Bosanquet-type effective viscosity model (Li et al., 2011), and the MRT-LBM results with effective viscosity correction (Guo et al., 2008). The Boltzmann equation is derived from the gas kinetic theory and fits all flow regimes ranging from the continuum flow regime to the free-molecule flow regime. The MRT-LBM model acts as a numerical solver to the Boltzmann equation with finite velocities. In fact, it recovers the Navier-Stokes equations by applying the multi-scale analysis, whereas incorporating the effective viscosity correction into the MRT-LBM model for further capturing the Knudsen layer enables it to accurately model the micro-gaseous flow in the transition flow regime within a straight long-channel (Guo et al., 2008; Li et al., 2011).

Fig. 1 presents a comparison of the calculated results obtained by DM and DBB and the predominately reported results (Hadjiconstantinou, 2003; Cercignani et al., 2004; Guo et al., 2008; Li et al., 2011). As expected, the Navier-Stokes solution with the velocity-slip boundary (Hadjiconstantinou, 2003), despite matching well with the existing results in the continuum and near-continuum flow regimes, noticeably deviates from the solutions of the Boltzmann equation (Cercignani et al., 2004) in the

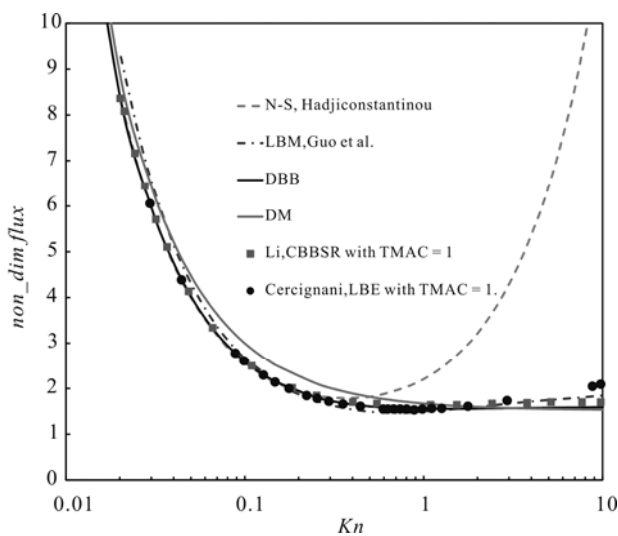


Fig. 1. The relationship of non-dimensional mass flow rate and Knudsen number.

The results are compared with existing results (Hadjiconstantinou, 2003; Cercignani et al., 2004; Guo et al., 2008; Li et al., 2011).

transition flow regime when $Kn > 0.3$, beyond which the continuum hypothesis and Navier-Stokes equations fail. Good agreement is found between the DBB results and those of Guo et al. (Guo et al., 2008), Li et al. (Li et al., 2011), as well as the solution of the Boltzmann equation (Cercignani et al., 2004). The DM results are slightly larger than those cited in the references (Hadjiconstantinou, 2003; Cercignani et al., 2004; Li et al., 2011) in the slip and early transition flow regimes, which is acceptable.

To further validate the DM and DBB boundaries, we compute the streamwise velocity at the wall surface and the channel centerline. The streamwise velocity is regularized as $U = u/u_{ave}$, with $u_{ave} = 1/H \int_0^H u dy$. In this part, DSMC results and the solution of the linearized Boltzmann equation (BE) are included for detailed comparison. As stated in the introduction, the DSMC can be viewed as a numerical strategy to directly solve the Boltzmann equation by utilizing a series of artificial particles to model real gas molecules without introducing many hypotheses, such as the law of gas-solid interaction, and the streaming and collisions of molecules. Considering that the Boltzmann equation derived from the gas kinetic theory can be employed to describe the rarefied gas flow at high Kn , where the Navier-Stokes equations break down, the DSMC can act as a more mature and accurate solver for the rarefied gas flow compared to the MRT-LBM model and Navier-Stokes equations (Verhaeghe et al., 2009), even though it suffers from expensive computational costs in modeling low velocity micro-flows. Fig. 2 presents the comparisons between the predicted velocity obtained by the present MRT-LBM and the existing results. The calculated velocity at the channel centerline with the DM and DBB boundary matches well with DSMC results and linearized BE results (Suga, 2013), while the predicted velocity at the wall's surface is slightly larger than the DSMC and linearized BE results in slip and transition flow regimes. Overall, according to our comparisons the present MRT-LBM with corrected effective viscosity can sufficiently capture the micro-

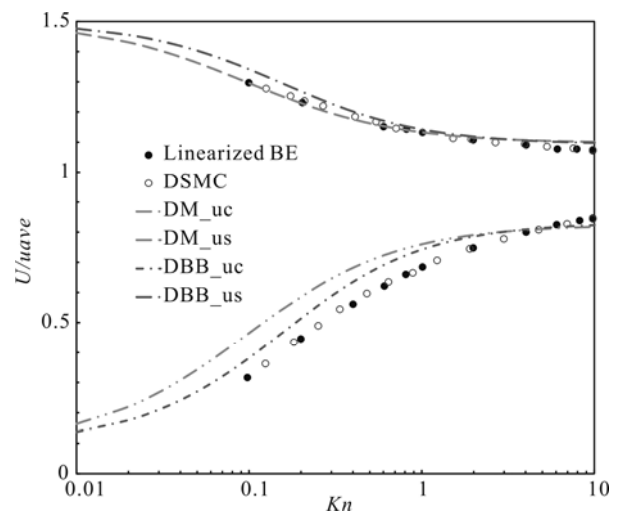


Fig. 2. The predicted velocity at the wall surface and channel centerline by DM and DBB boundary, respectively. The results are compared with existing results (Suga, 2013).

gaseous flow in the slip and transition flow regimes in a straight long-channel.

In the above validation cases, the micro-gaseous flow is driven by a constant external force $\partial p / \partial x = 10^{-4}$. This does not reveal the real conditions in shale reservoirs, where gas flows are generally driven by the pressure gradient, rather than a constant external force. As pointed out above, the Knudsen number is a pressure-dependent parameter in this condition. Therefore, we conduct the validation cases with micro-gaseous flow driven by the pressure gradient in a long micro-channel in this section. The micro-gaseous flow is driven by a pressure difference between the inlet boundary (higher pressure p_{in} or density ρ_{in}) and outlet boundary (lower pressure p_{out} or density ρ_{out}). Considering the straight channel with constant local characteristic length for every node, the local Knudsen number can be calculated according to Section 2.3:

$$Kn(x) = \frac{Kn_{out} p_{out}}{p(x)} = \frac{Kn_{in} p_{in}}{p(x)},$$

where Kn_{in} and Kn_{out} are the Knudsen number at inlet boundary and outlet boundary, respectively, and $p(x)$ is the pressure along the channel. The basic set-up for this validation model is: 1) the lattice size is set as $N_x=2000$ and $N_y=20$ to maintain consistence with the previous study (Li et al., 2011), namely, the ratio of length over width equals to 100; 2) the ratio of inlet pressure p_{in} over outlet pressure p_{out} is set as 1.4 for $Kn_{out} = 0.0194$, while $p_{in}/p_{out}=2.0$ for $Kn_{out} = 0.194, 0.388$; 3) the inlet and outlet boundaries are the pressure boundary proposed by Luo et al. (Verhaeghe et al., 2009); 4) the slip boundary schemes (DM and DBB) introduced in Section 2.2 are exerted on the top and bottom walls.

The calculated results by DM and DBB schemes are presented in Figs. 3 to 5, where the streamwise velocity at the outlet is defined as u/u_{max} , with u_{max} being the maximum streamwise velocity at the outlet, and the

pressure deviation distribution along channel is given by $\delta p = (p(x) - p_i) / p_{out}$, $p_i = p_{in} + (p_{out} - p_{in})x/L$. The DSMC and information-preservation direct simulation Monte Carlo (IP-DSMC) results (Shen et al., 2004), the results of Luo et al. (Verhaeghe et al., 2009), and the results of Arkilic et al. (Arkilic et al., 1997) are also included in these figures for better comparison. As mentioned above, direct simulation of the Monte Carlo method directly solves the Boltzmann equation to model micro-flows, thereby presenting a more reliable and accurate results. Thus, in this section, the results from DSMC and IP-DSMC serve as benchmarking cases. The results of Luo et al. (Verhaeghe et al., 2009) are predicted by the MRT-LBM model combined with the first-order velocity-slip boundary. In fact, the model of Luo et al. is equivalent to the incompressible Navier-Stokes equations with the first-order slip boundary scheme (Verhaeghe et al., 2009). The study of Arkilic et al. (Arkilic et al., 1997) presents analytical results for the compressible Navier-Stokes equations with first-order velocity-slip boundary scheme.

Figs. 3 to 5 show the predicted streamwise velocity and non-dimensional pressure distribution by the DM and DBB scheme. The velocity predicted by DM matches well with the DSMC and IP-DSMC results (Shen et al., 2004), and the pressure deviation along the long-channel also agrees well with the DSMC and IP-DSMC results for $Kn=0.0194, 0.194, 0.388$, although slight differences are observed in the pressure deviation at $Kn=0.388$. Both the velocity profiles and pressure deviation calculated by the DBB boundary show good agreement with the DSMC and IP-DSMC results for three different Kn . A detailed comparison between Figs. 3 to 5 indicates that the DBB scheme is superior to the DM scheme in predicting micro-gaseous flow in slip and early transition flow regimes in a straight channel. The velocity predicted by Luo et al. and Arkilic et al. agrees well with the DSMC and IP-DSMC results for $Kn=0.0194, 0.194$, as the Kn increases, it gradually deviates from the DSMC and IP-DSMC results. The pressure deviation from both Luo et al. and Arkilic et

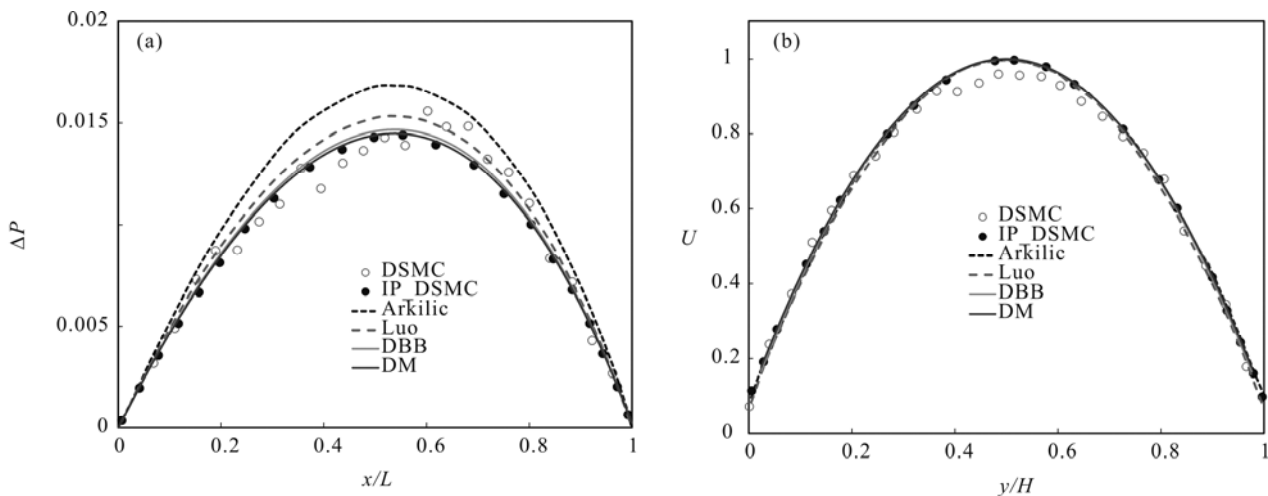


Fig. 3. The predicted streamwise velocity at outlet and pressure deviation distribution along channel by DM and DBB scheme when micro-gaseous flow is driven by pressure gradient for $Kn_{out} = 0.0194$.

The results are compared with existing results: DSMC and IP-DSMC results (Shen et al., 2004), Luo et al. (Verhaeghe et al., 2009), and Arkilic et al. (Arkilic et al., 1997): (a) streamwise velocity, (b) pressure deviation distribution along channel.

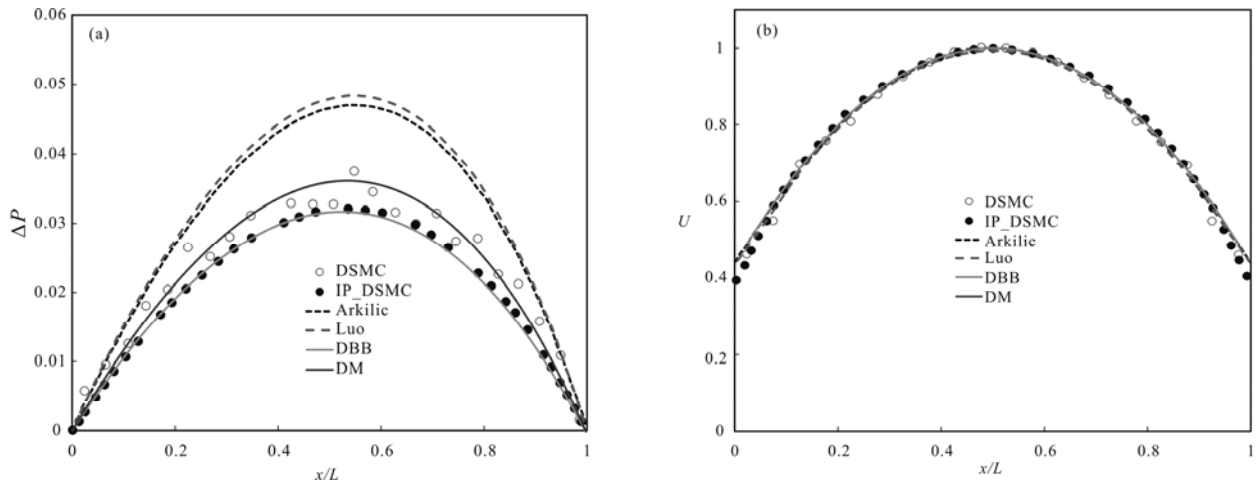


Fig. 4. The predicted streamwise velocity at outlet and pressure deviation distribution along channel by DM and DBB scheme when micro-gaseous flow is driven by pressure gradient for $Kn_{out} = 0.0194$.

The results are compared with existing results: DSMC and IP-DSMC results (Shen et al., 2004), Luo et al. (Verhaeghe et al., 2009), and Arkilic et al. (Arkilic et al., 1997): (a) streamwise velocity, (b) pressure deviation distribution along channel.

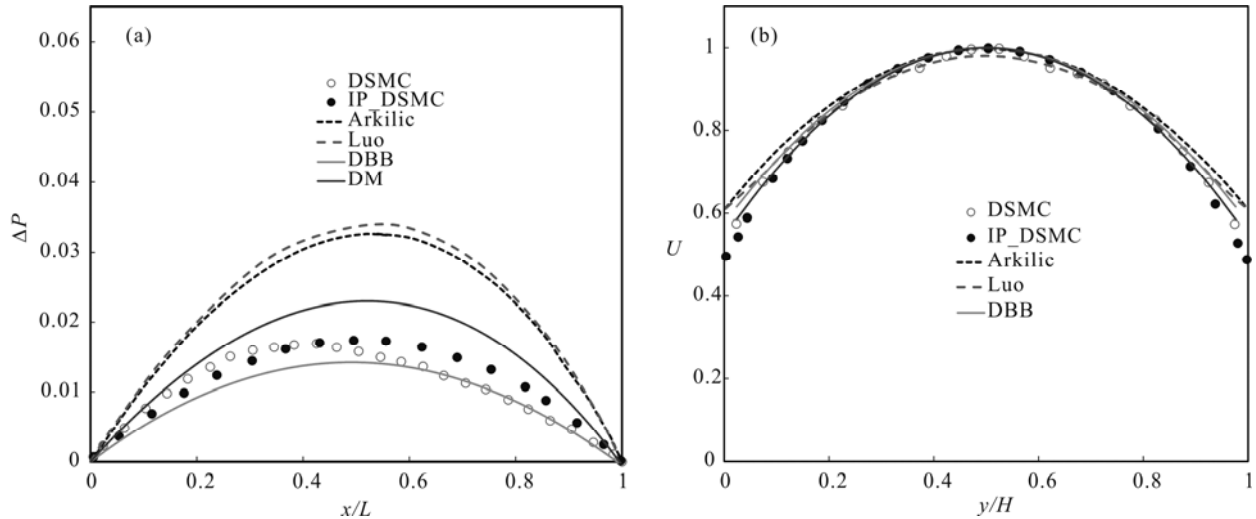


Fig. 5. The predicted streamwise velocity at outlet and pressure deviation distribution along channel by DM and DBB scheme when micro-gaseous flow is driven by pressure gradient for $Kn_{out} = 0.388$.

The results are compared with existing results: DSMC and IP-DSMC results (Shen et al., 2004), Luo et al. (Verhaeghe et al., 2009), and Arkilic et al. (Arkilic et al., 1997): (a) streamwise velocity, (b) pressure deviation distribution along channel.

al. matches with the DSMC and IP-DSMC results at $Kn=0.0194$, however, the discrepancies between them happen at $Kn = 0.194, 0.388$ and gradually become more noticeable as the Kn increases. Additionally, the results between Luo et al. and Arkilic et al. show little difference when $Kn=0.0194, 0.194, \text{ and } 0.388$. This is because the Luo et al. and Arkilic et al. models are equivalent to the incompressible and compressible Navier-Stokes equations, respectively, which are not sufficient for modeling the transition flow regime and free-molecule flow regime ($Kn>0.1$) where the continuum-based Navier-Stokes equations are not valid. Although the present MRT-LBM models with the DBB and DM scheme are also actually equivalent to Navier-Stokes equations with the velocity-slip boundary, the introduction of Bosanquet-type effective viscosity in Section 2 extends the MRT-LBM model to the transition flow regime ($0.1<Kn<10$) in the

straight long-channel. The fact that the predicted results by Luo et al. and Arkilic et al. via Navier-Stokes equations with first-order velocity-slip boundary overestimate the velocity at the walls for the case with $Kn=0.388$ can also be attributed to the absence of effective viscosity correction for accurately capturing the Knudsen layer, in which the mean free path of gas molecules is reduced, and effective viscosity is not constant due to the wall effects. Considering the effects of the Knudsen layer, the effective viscosity of the gas is actually smaller than its dynamic viscosity determined by the mean free path of gas molecules in the unbounded space, which will lead to a larger streamwise velocity at the channel centerline, and thereby a smaller normalized streamwise velocity u/u_{max} at the wall, as shown in Fig. 5(a).

As the Knudsen number increases, the microscale effect and rarefaction effect become more obvious and require to

be carefully addressed. In the following validation, the rarefaction and microscale effects on micro-gaseous flow in the long-channel are further studied. The calculated non-dimensional flux is compared to the existing experimental results reported by Colin et al. (Colin et al., 2004; Colin, 2005) and Maurer et al. (Maurer et al., 2003), the analytical results obtained by the first-order velocity-slip model of Arkilic et al. (Arkilic et al., 1997), and the analytical solution of the second-order velocity-slip model of Aubert and Colin (Aubert and Colin, 2001). The experiments (Maurer et al., 2003; Colin et al., 2004; Colin, 2005) have been conducted with high accuracy to predict the rarefied gas flows at a moderate Knudsen number. In order to compare with the experimental results, the ratio of inlet pressure p_{in} over outlet pressure p_{out} is set as 1.8. The non-dimensional flux is defined as $S = m/m_{ns}$, where the flux m is calculated by the present MRT-LBM considering the microscale and rarefaction effect (given by Equation (2.11)), and m_{ns} is the flux in the continuum assumption with non-slip boundary. The flux can be given as follows (Maurer et al., 2003)

$$m_{ns} = \frac{\Delta P p_m b^3}{12 \mu p_{out} L}, \quad (2.27)$$

$$P_m = (p_{in} + p_{out})/2, \Delta P = p_{in} - p_{out}$$

where p_{in} is the inlet pressure, p_{out} is the outlet pressure, μ is the dynamic viscosity of the fluid, b is the channel width, and L is the channel length along the streamwise direction.

Fig. 6 presents the non-dimensional flux and its reciprocals that vary with the Knudsen number. The non-dimensional flux, predicted by DBB scheme, is slightly lower than that predicted by DM scheme, and it can be observed that the predicted results by both the DBB and the DM scheme match with the experimental results reported by Colin et al. (Colin et al., 2004; Colin, 2005) and Maurer et al. (Maurer et al., 2003), indicating that the present MRT-LBM with effective viscosity and velocity-slip boundary scheme (DBB and DM boundary) can effectively capture the microscale and rarefaction effects of micro-gaseous flow in the long-channel for slip and early transition flow regimes. A comparison between the

experimental results and the results of Arkilic et al. and Aubert et al. indicates that the first-order slip theory and second-order slip model underestimates and overestimates the flux at moderate Knudsen number, respectively, which is in accordance with the results of Hadjiconstantinou et al. (Hadjiconstantinou, 2003).

The above validations demonstrate that the present MRT-LBM model can effectively capture the microscale flow in a long-channel for slip and transition flow regimes. However, whether the corrected effective viscosity based on a straight long-channel can be directly extended into the cases involving complicated boundary remains a puzzle and has not been well addressed to date. In what follows, we apply this MRT-LBM to model the micro-gaseous flow in complex porous media and then compare to the results obtained by Su et al. (Su et al., 2017), Wu et al. (Wu et al., 2017), and Liu et al. (Liu et al., 2018), who numerically solve the linearized BGK equation via the discrete velocity method to capture the micro-gaseous flow in complicated porous media, pointing out some limitations and inaccuracies of the present MRT-LBM method.

3 Discussions

Although LBM models originate from the kinetic theory of molecules (Succi, 2001; Guo and Shu, 2013) and can be considered as a simple discrete form of the Boltzmann equation that is derived at the mesoscopic scale, the MRT-LBM, actually, is a continuum-based computational fluid dynamics solver because the Navier-Stokes can be recovered from MRT-LBM model under the low Mach number assumption (Guo and Shu, 2013). Despite extensive valuable attempts by previous studies (Zhang et al., 2006; Guo et al., 2007b; Guo and Zheng, 2008; Guo et al., 2008; Tang et al., 2008) that have extended its application to the transition flow regime and free-molecular flow regime, in most circumstances, these models are derived based on straight channels and only verified by micro-Poiseuille flow in straight long-channels. Whether these models can be directly extended to simulate transition flow regime in complicated porous

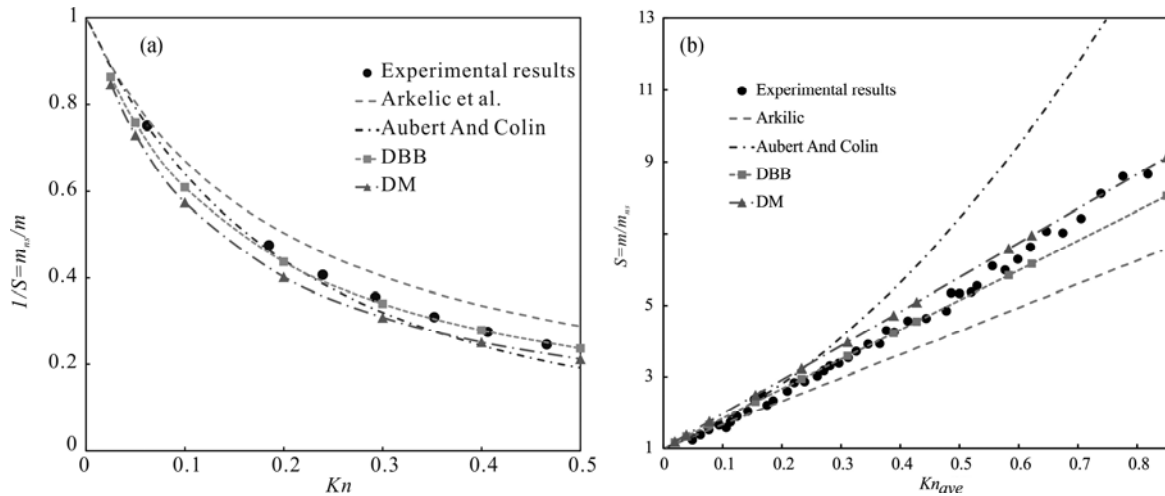


Fig. 6. The non-dimensional flux of micro-gaseous flow in long-channel with Knudsen number over a wide range. The results predicted by DM and DBB boundary are compared with existing results: Colin et al. (Colin et al., 2004; Colin, 2005), Maurer et al. (Maurer et al., 2003), and Arkilic et al. (Arkilic et al., 1997): (a) $1/S = m_{ns}/m$, (b) $S = m/m_{ns}$.

media remains less understood. In this section, we focus on the lattice Boltzmann modeling of the micro-gaseous flow in slip and transition flow regimes in the porous media reported in previous studies (Su et al., 2017; Wu et al., 2017), and conduct the detailed comparisons between the results predicted by the present MRT-LBM and the encouraging results of Wu et al. (Su et al., 2017; Wu et al., 2017), who accurately solved the numerical results of the linearized BGK equation with DVM to predict the rarefied gas flows in complex porous media. Both DVM and LBM numerically solve the simplified Boltzmann equation with a series of discrete velocities (Su et al., 2017). The LBM models, including single relaxation time LBM (SRT-LBM), MRT-LBM, and other high-order LBM models, can be regarded as the special forms of the DVM model because of a set of fixed velocities with high isotropy in use. A large number of velocities are required to capture rarefied gas flows because of the large variations and discontinuities in the particle distribution function (Su et al., 2017), which is beyond the scope of the MRT-LBM models due to fixed velocities. Thus, the DVM is superior to the LBM models in predicting the rarefied gas flow with large Knudsen number, although it is time-consuming and expensive. Based on the existing results by accurately solving the simplified Boltzmann equation via DVM, we finally point out some limitations of the present MRT-LBM model and obtain an approximate critical Knudsen number, below which the present MRT-LBM model behaves well.

Fig. 7 presents three random porous media used in this study and a previous study (Su et al., 2017): a channel filled with random rocks (media 1), a channel filled with squares (media 2), and a channel filled with circles (media 3). The micro-gaseous flows in three porous media are conducted at different Knudsen numbers ranging from 0.01 to 10, which covers the majority of micro-gaseous flows in slip and transition flow regimes. The computational model is set as follows: 1) the left boundary (high pressure) and right boundary (low pressure) are the ZouHe pressure boundary scheme (Zou and He, 1997); 2) the top boundary, bottom boundary, and the surface of solids are the DM boundary and DBB boundary given in the above sections; 3) for modeling of the micro-gaseous flow in the transition flow regime, we introduce the Bosanquet-type effective viscosity to capture the rarefaction effects; 4) other parameters are consistent with Su et al. (Su et al., 2017) and Wu et al. (Wu et al., 2017).

Fig. 8 shows the detailed velocity vectors of micro-gaseous flow in media 2 at different Knudsen numbers. As expected, as the Knudsen number increases, the slip velocity at walls increases, and the small pores contribute to a large amount of mass flux due to the larger Knudsen number. Subsequently, we calculate the non-dimensional permeability and compare to the DVM results (Su et al., 2017; Wu et al., 2017), as shown in Fig. 9. The apparent permeability K_a calculated by this MRT-LBM considers the microscale and rarefaction effects, and the absolute permeability K_{abs} corresponds to the results in the continuum limit without these effects. Figs. 9(a) and 9(b) present the non-dimensional permeability predicted by the DM boundary and DBB boundary, respectively, and the

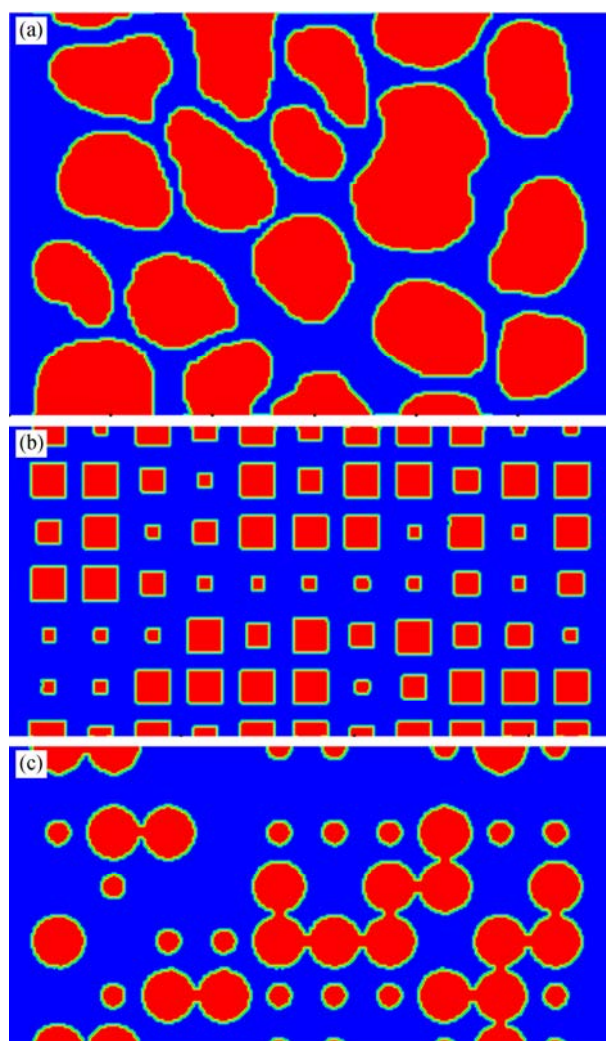


Fig. 7. Three porous media used in this simulation are consistent with those of Su et al. (Su et al., 2017): (a) media 1; (b) media 2; (c) media 3.

DVM results from Su et al. (Su et al., 2017) are also included in these subfigures for better comparison.

The comparisons indicate that the MRT-LBM model combined with the DM and DBB boundary substantially underestimates the permeability in comparison to the DVM when the Knudsen number is larger than 1.0. Hence, the MRT-LBM model, despite considering the rarefaction effect by correcting the effective viscosity, still cannot accurately capture micro-gaseous flow in complicated porous media in the transition flow regime where $Kn > 1.0$. Therefore, the Bosanquet-type effective viscosity derived according to straight long-channels (Beskok and Karniadakis, 1999) is not suitable for other complicated porous media. Despite numerous models proposed for the effective viscosity in existing studies (Zhang et al., 2006; Guo et al., 2007b; Guo and Zheng, 2008; Guo et al., 2008; Tang et al., 2008), nearly all of them are only applicable for simple geometries, and their effectiveness is only validated with the micro-Poiseuille flow. The direct extension of their applications to random porous media might become problematic. This is also

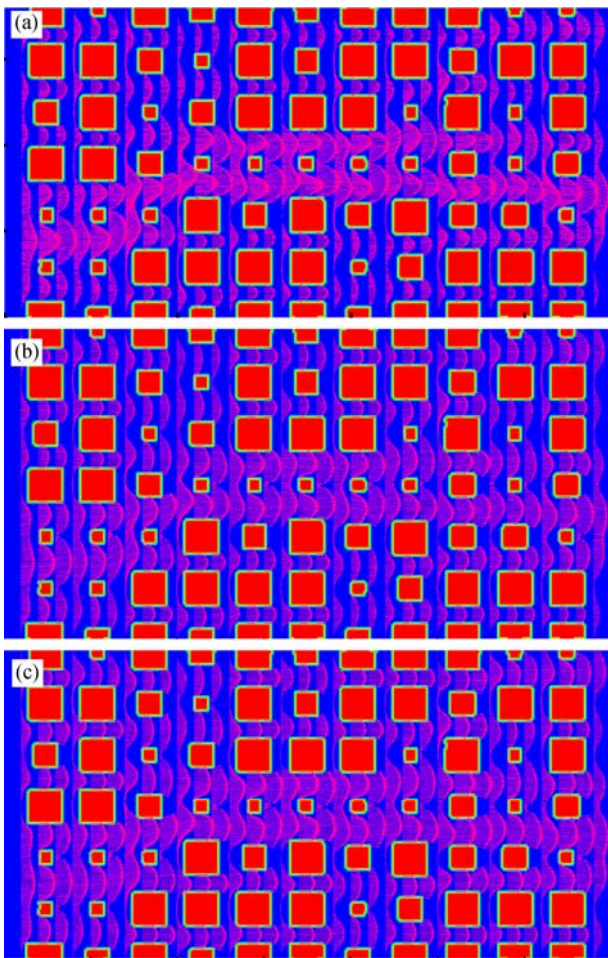


Fig. 8. The velocity vectors of micro-gaseous flow in media 2 under different Knudsen numbers: (a) $Kn=0.01$; (b) $Kn=0.5$; (c) $Kn=5.0$. The results are predicted by DBB boundary scheme

verified by the study of Liu et al. (Liu et al., 2018), who recently investigated the rarefaction throttling effect by the discrete velocity method, revealing that the case involving

the bend channel is more complicated than the straight channel, and it is influenced not only by the rarefaction effect, but also by the bend angle as well as the shape and configuration of channels. We further validate the accuracy and effectiveness of this MRT-LBM by the comparison with the numerical solution of the linearized BGK equation given by Wu et al. (Wu et al., 2017), who accurately calculated the apparent permeability of the micro-gaseous flow in the channel filled with circles and squares, as shown in Fig. 10. Figs. 11 to 12 present the velocity vectors of the micro-gaseous flow in two porous media. Both the pore structures and the velocity vector of the micro-gaseous flow exhibit a great difference in the channel filled with circles and squares. However, as depicted in Figs. 13 and 14, the predicted permeability with the DBB and DM boundary cannot effectively identify this difference. For the channel filled with circles, the calculated permeability with the DBB and DM boundary is in agreement with that predicted by accurately solving the linearized BGK equation, while the large discrepancy between them is observed for the large Knudsen number flows in the channel filled with squares. The comparisons indicate that the Bosanquet-type effective viscosity derived from the straight channel, despite being capable of capturing the rarefied gas flow in the transition flow regime in the straight long-channel, cannot to be directly extended to other complicated boundaries to simulate micro-flows with a large Knudsen number in irregular micro/nano-pores. Unfortunately, nearly all viscosity correction models for capturing micro-flows in the transition flow regime are built based on the straight channel. Moreover, it is a challenging task to establish a reliable and united model for the effective viscosity correction to address the high Knudsen-number flows resulting from the complexity of porous media. Thus, it is critical to determine the flow regimes in which the MRT-LBM models or Navier-Stokes equations combined with corrected viscosity and velocity-slip boundary schemes provide reliable results.

In order to approximately obtain a critical Knudsen number, at which the MRT-LBM provides more accurate

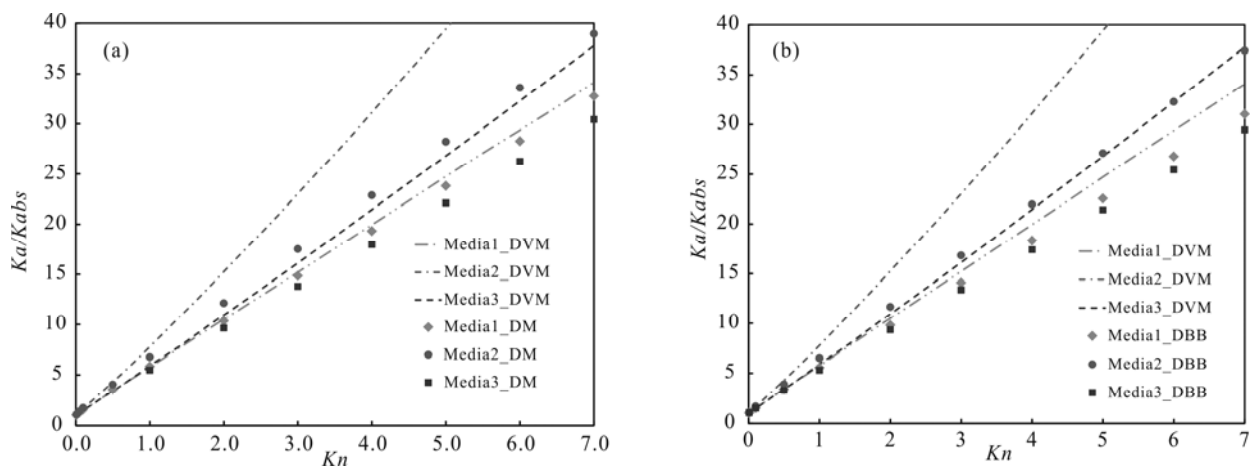


Fig. 9. The non-dimensional permeability of micro-gaseous flow in three porous media with Knudsen number over a wide range from 0.01 to 7. A detailed comparison between the predicted results by the present DM and DBB schemes and discrete velocity method in Su et al.'s study (Su et al., 2017): (a) DM boundary scheme; (b) DBB boundary scheme.

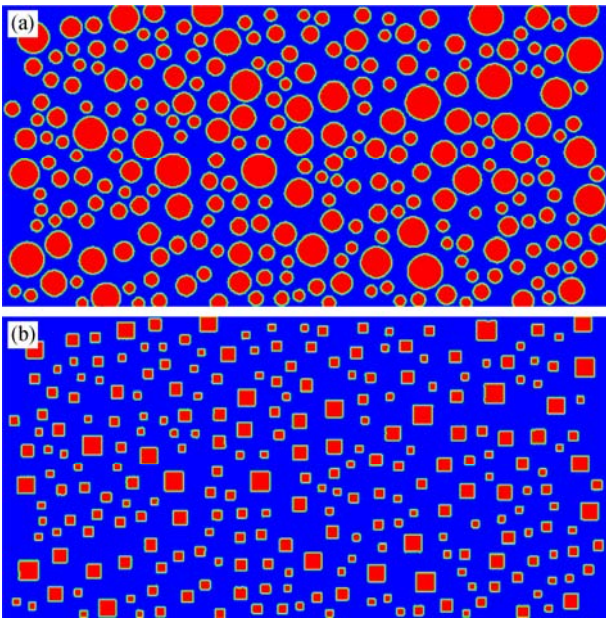


Fig. 10. Two porous media used in Wu et al.'s study (Wu et al., 2017), who simulated the micro-gaseous flow in complicated porous media in slip and transition flow regimes by accurately solving the linearized BGK equation: (a) channel filled with circles; (b) channel filled with squares.

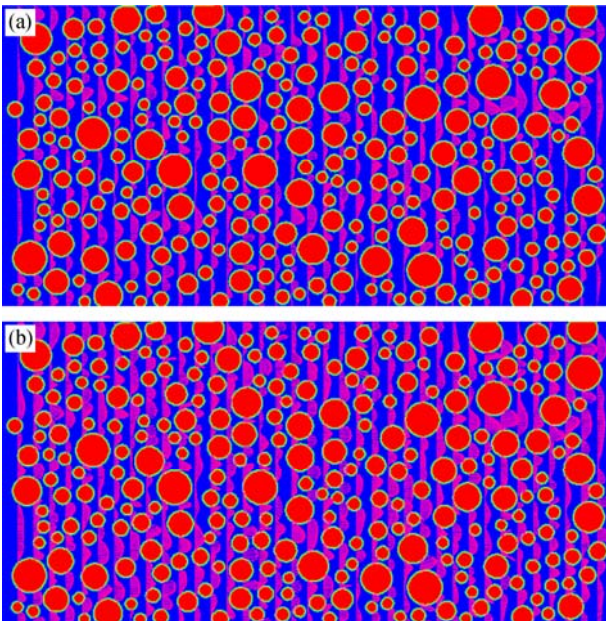


Fig. 11. The velocity vectors of micro-gaseous flow in the channel filled with circles under different Knudsen numbers: (a) $Kn=0.01$; (b) $Kn=4.0$. The results are predicted by DM boundary.

results, we further model the micro-gaseous flow for $Kn < 0.5$ in the same porous media. Figs. 13 to 15 depict the non-dimensional permeability of micro-gaseous flow in several porous media with the Knudsen number ranging from 0.0 to 0.5. From these figures, we can observe that the MRT-LBM results start to deviate from the DVM results or the numerical solutions of the linearized BGK equation when the Knudsen number is larger than 0.3.

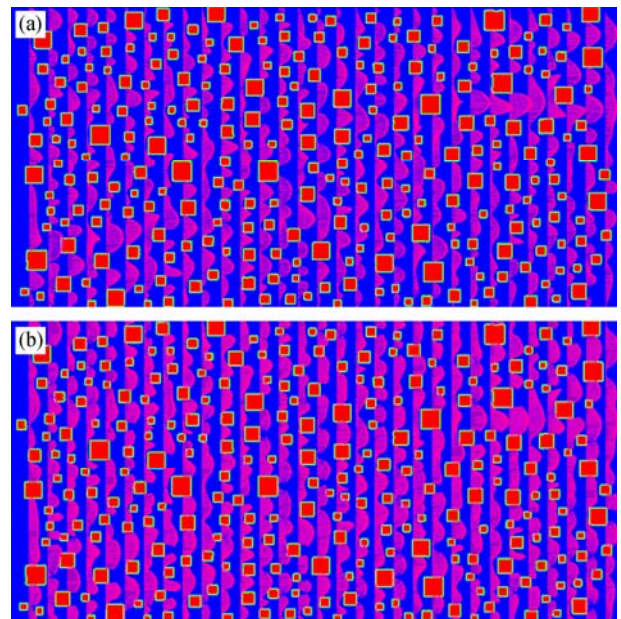


Fig. 12. The velocity vectors of micro-gaseous flow in the channel filled with squares under different Knudsen numbers: (a) $Kn=0.01$; (b) $Kn=4.0$. The results are predicted by DM boundary.

Thus, as a continuum-based solver, the MRT-LBM combined with the corrected effective viscosity can effectively simulate the gas flow in complicated porous media in the continuum flow regime, slip flow regime, and early transition flow regime when $Kn < 0.3$. Nevertheless, the MRT-LBM remains less accurate for modeling of the micro-gaseous flow in complex reservoirs at a large Knudsen-number.

4 Conclusions

In this study, we validate the effectiveness of the MRT-LBM combined with the DM and DBB boundary in the modeling of micro-gaseous flow in several porous media reported in previous studies (Su et al., 2017; Wu et al., 2017) within slip and transition flow regimes. We conduct a detailed comparison between the predicted results with the DM and DBB boundary and those predicted by DVM (Su et al., 2017; Wu et al., 2017), revealing some limitations of the present MRT-LBM with regard to the prediction of micro-gaseous flow in complicated porous media. To capture the large Knudsen-number flows, the Bomanquet-type effective viscosity is employed to consider the rarefaction effect. Based on these results, the following conclusions are drawn:

(1) The popular kinetic boundary conditions for the LBM modeling of micro-gaseous flow are the discrete Maxwellian (DM) boundary, the combined diffusive reflection and bounce-back scheme (DBB), and the combined bounce-back scheme and specular reflection (BSR). The BSR boundary can only be applicable for the straight or regular channel, as it relies on the normal direction of walls, while the DM and DBB boundary have good adaptability to curved walls.

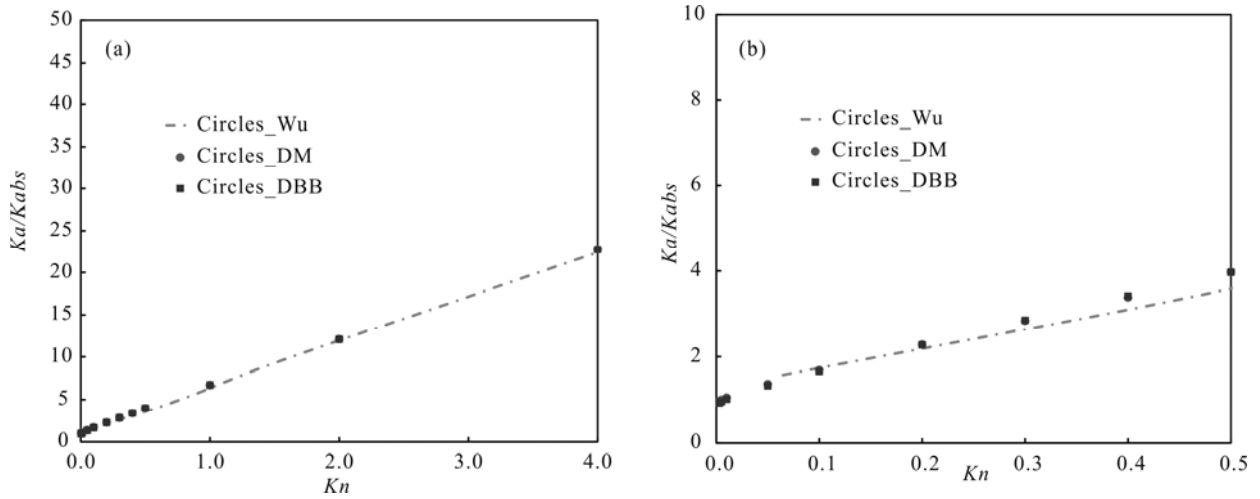


Fig. 13. The non-dimensional permeability of micro-gaseous flow in the channel filled with circles with Knudsen number over a wide range from 0.0 to 4.0. A detailed comparison between the predicted results by this DM and DBB and numerical results of the linearized BGK equation (Wu et al., 2017): (a) $Kn=0.0-4.0$; (b) $Kn=0.0-0.5$.

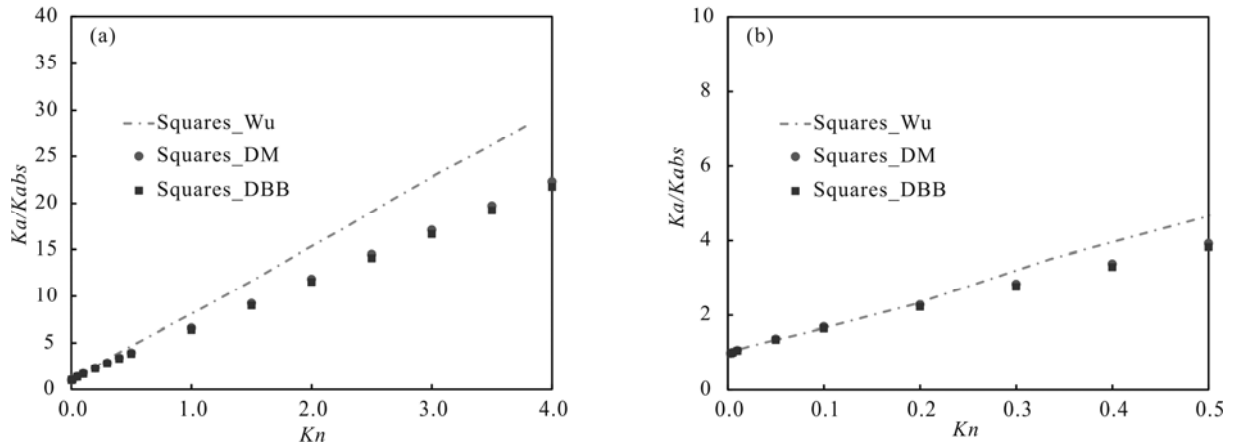


Fig. 14. The non-dimensional permeability of micro-gaseous flow in the channel filled with squares with Knudsen number over a wide range from 0.0 to 4.0. A detailed comparison between the predicted results by this DM and DBB and numerical results of the linearized BGK equation (Wu et al., 2017): (a) $Kn = 0.0-4.0$; (b) $Kn = 0.0-0.5$.

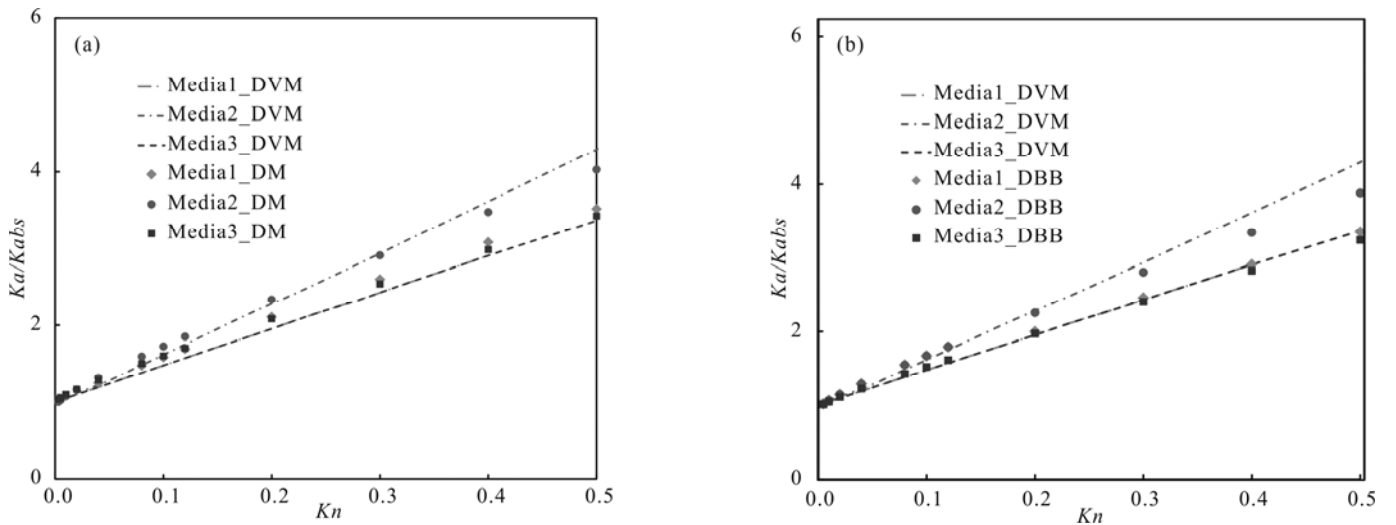


Fig. 15. The non-dimensional permeability of micro-gaseous flow in three porous media (Su et al., 2017) with Knudsen number over a wide range from 0.0 to 0.5. A detailed comparison of the predicted results by this DM and DBB and those by discrete velocity method in Su et al.'s works (Su et al., 2017): (a) DM boundary scheme, (b) DBB boundary scheme.

(2) While modeling the micro-gaseous flow in complicated porous media, the MRT-LBM provides good predictions for the straight channel, while underestimating the permeability compared to that obtained by the DVM for large Knudsen-number flows. This indicates that the Bosanquet-type effective viscosity derived from a straight long-channel has extremely limited applicability to other complicated porous media. Thus, the direct extension of effective viscosity derived from a straight long-channel to random porous media might become problematic. A detailed comparison of MRT-LBM and DVM results, as well as numerical solutions of linearized BGK equations indicates that the present MRT-LBM combined with the corrected effective viscosity is capable of providing reliable results when the Knudsen number is less than 0.3.

In conclusion, the MRT-LBM, as a continuum-based CFD solver in nature, can effectively model the micro-gaseous flow in complicated porous media in slip and early transition flow regimes when $Kn < 0.3$. It is also a challenging task to establish a reliable model for the effective viscosity correction that fits curved boundary to further address the high Knudsen-number flows in complicated porous media, which deserves our further research.

Acknowledgement

The proposed methodology in this paper is supported by the Strategic Program of Chinese Academy of Sciences (Grant No. XDB10030400), the Hundred Talent Program of Chinese Academy of Sciences (Grant No. Y323081C01) and The National Natural Science Fund (Grant No. 51439008). The authors would like to express their deepest gratitude for the generous support.

Manuscript received Nov. 19, 2018
accepted Feb. 4, 2019
associate EIC ZHANG Shuichang
edited by LIU Lian

References

- Ansumali, S., and Karlin, I.V., 2002. Kinetic boundary conditions in the lattice Boltzmann method. *Physical Review E*, 66: 026311.
- Arkilic, E.B., Schmidt, M.A., and Breuer, K.S., 1997. Gaseous slip flow in long microchannels. *Journal of Microelectromechanical Systems*, 6(2): 167–178.
- Aubert, C., and Colin, S., 2001. High order boundary conditions for gaseous flows in rectangular microducts. *Microscale Thermophysical Engineering*, 5(1): 41–54.
- Beskok, A., and Karniadakis, G. E., 1999. A model for flows in channels, pipes and ducts at micro- and nano-scales. *Microscale Thermophysical Engineering*, 3.
- Bird G.A., 1994. *Molecular gas dynamics and the direct simulation of gas flows*, Clarendon Press, Oxford, 1–479.
- Cercignani, C., Lampis, M., and Lorenzani, S., 2004. Variational approach to gas flows in microchannels. *Physics of Fluids*, 16(9): 3426–3437.
- Chai, Z.H., Guo, Z.L., Zheng, L., and Shi, B.C., 2008. Lattice Boltzmann simulation of surface roughness effect on gaseous flow in a microchannel. *Journal of Applied Physics*, 104(1): 5–16.
- Chai, Z.H., Shi, B.C., Guo, Z.L., and Lu, J.H., 2010. Gas flow through square arrays of circular cylinders with Klinkenberg effect: a lattice Boltzmann study. *Communications in Computational Physics*, 8(5): 1052–1073.
- Chapman, S., and Cowling, T.G., 1953. *The mathematical theory of non-uniform gases*. Cambridge University Press, 1–448.
- Chen, L., Jiang, Z.X., Liu, K.Y., Gao, F.L., and Wang, P.F., 2017. A combination of N₂ and CO₂ adsorption to characterize nanopore structure of organic-rich lower Silurian shale in the upper Yangtze platform, South China: implications for shale gas sorption capacity. *Acta Geologica Sinica (English Edition)*, 91(04):1380–1394.
- Chen X.D., and Hu G.Q., 2015. Multiphase flow in microfluidic devices. *Chinese Journal of Theoretical and Applied Mechanics*, 47(02):384 (in Chinese with English abstract).
- Christou, C., and Dadzie, S.K., 2016. Direct-simulation Monte Carlo investigation of a Berea porous structure. *SPE Journal*, 21(3): 938–946.
- Colin, S., 2005. Rarefaction and compressibility effects on steady and transient gas flows in microchannels. *Microfluidics and Nanofluidics*, 1(3): 268–279.
- Colin, S., Lalonde P., and Caen R., 2004. Validation of a second-order slip flow model in rectangular microchannels. *Heat Transfer Engineering*, 25(3): 23–30.
- Cudjoe, S., and Barati, R., 2017. Lattice Boltzmann Simulation of CO₂ Transport in Kerogen Nanopores—An Evaluation of CO₂ Sequestration in Organic-Rich Shales. *Journal of Earth Science*, 28(5): 926–932.
- Ge, M.N., Ren, S.M., Guo, T.X., Zhou, Z., Wang, S.J., and Bao, S.J., 2016. Characterizing the micropores in Lacustrine shales of the Late Cretaceous Qingshankou formation of southern Songliao Basin, NE China. *Acta Geologica Sinica (English Edition)*, 92(06):2267–2279.
- Geng, L.D., Li, G.S., Zitha, P., Tian, S.C., Sheng, M., and Fan, X., 2016. A diffusion-viscous flow model for simulating shale gas transport in nano-pores. *Fuel*, 181: 887–894.
- Guo, Z.L., Shi, B.C., Zhao, T.S., and Zheng, C.G., 2007a. Discrete effects on boundary conditions for the lattice Boltzmann equation in simulating microscale gas flows. *Physical Review E*, 76: 056704.
- Guo, Z.L., Shi, B.C., and Zheng, C.G., 2007b. An extended Navier-Stokes formulation for gas flows in the Knudsen layer near a wall. *Europhysics Letters*, 80(2): 24001.
- Guo, Z.L., and Shu, C., 2013. *Lattice Boltzmann method and its applications in engineering*. Singapore, World Scientific Publishing Co. Pte. Ltd, 1–419.
- Guo, Z.L., Zhao, T.S., and Shi, Y., 2006. Physical symmetry, spatial accuracy, and relaxation time of the lattice Boltzmann equation for microgas flows. *Journal of Applied Physics*, 99(7): 074903-1–074903-8.
- Guo, Z.L., and Zheng, C.G., 2008. Analysis of lattice Boltzmann equation for microscale gas flows: Relaxation times, boundary conditions and the Knudsen layer. *International Journal of Computational Fluid Dynamics*, 22(7): 465–473.
- Guo, Z.L., Zheng, C.G., and Shi, B.C., 2008. Lattice Boltzmann equation with multiple effective relaxation times for gaseous microscale flow. *Physical Review E*, 77(3): 036707.
- Hadjicostantinou, N.G., 2003. Comment on Cercignani's second-order slip coefficient. *Physics of Fluids*, 15(8): 2352–2354.
- Landry, C.J., Prodanović, M., and Eichhubl, P., 2016. Direct simulation of supercritical gas flow in complex nanoporous media and prediction of apparent permeability. *International Journal of Coal Geology*, 159: 120–134.
- Latt, J., and Chopard, B., 2006. Lattice Boltzmann method with regularized pre-collision distribution functions. *Mathematics and Computers in Simulation*, 72(2): 165–168.
- Li, Q., He, Y.L., Tang, G.H., and Tao, W.Q., 2011. Lattice Boltzmann modeling of microchannel flows in the transition flow regime. *Microfluidics and Nanofluidics*, 10(3): 607–618.
- Lin, K., Yuan, Q.Z., and Zhao, Y.P., 2017. Using graphene to simplify the adsorption of methane on shale in MD simulations. *Computational Materials Science*, 133: 99–107.
- Liu, Huihai, Georgi, D., and Chen, J.H., 2018. Correction of source-rock permeability measurements owing to slip flow and Knudsen diffusion: a method and its evaluation. *Petroleum Science*, 15(1): 116–125.
- Liu, W., Tang, G.H., Su, W., Wu, L., and Zhang, Y.H., 2018. Rarefaction throttling effect: Influence of the bend in micro-

- channel gaseous flow. *Physics of Fluids*, 30: 12.
- Liu, X., Zhu, Y.F., Gong, B., Yu, J.P., and Cui, S.T., 2015. From molecular dynamics to lattice Boltzmann: a new approach for pore-scale modeling of multi-phase flow. *Petroleum Science*, 12(2): 282–292.
- Maurer, J., Tabeling, P., Joseph, P., and Willaime, H., 2003. Second-order slip laws in microchannels for helium and nitrogen. *Physics of Fluids*, 15(9): 2613–2621.
- Ning, Z.F., Wang, B., Yang, F., Zeng, Y., Chen, J.E., and Zhang, L., 2014. Microscale effect of microvoids in shale reservoirs. *Petroleum Exploration and Development*, 41(4): 492–499 (in Chinese with English abstract).
- Qian, Y.H., D'Humières, D., and Lallemand, P., 2007. Lattice BGK models for Navier-Stokes equation. *Europhysics letters*, 17(6): 479–484.
- Qiao, Y.C., Lei, X., Tian, Y., and Guo, Z.Q., 2013. Numerical simulation of the pollutants transport in Tai lake with lattice Boltzmann method. *Acta Geologica Sinica (English Edition)*, 87(supp.): 647–648.
- Shan, X.W., Yuan, X.F., and Chen, H.D., 2006. Kinetic theory representation of hydrodynamics: a way beyond the Navier–Stokes equation. *Journal of Fluid Mechanics*, 550(7): 413–441.
- Shen, C., Tian, D.B., Xie, C., and Fan, J., 2004. Examination of the LBM in simulation of microchannel flow in transitional regime. *Microscale Thermophysical Engineering*, 8(4): 423–432.
- Silin, D., and Patzek, T., 2006. Pore space morphology analysis using maximal inscribed spheres. *Physica A*, 371(2): 336–360.
- Su, W., Lindsay, S., Liu, H.H., and Wu, L., 2017. Comparative study of the discrete velocity and lattice Boltzmann methods for rarefied gas flows through irregular channels. *Physical Review E*, 96(2): 023309.
- Succi, S., 2001. *The lattice Boltzmann equation for fluid dynamics and beyond*. Oxford University Press, New York, 1–304.
- Succi, S., 2002. Mesoscopic modeling of slip motion at fluid–solid interfaces with heterogeneous catalysis. *Physical Review Letters*, 89(6): 064502.
- Suga, K., 2013. Lattice Boltzmann methods for complex microflows: applicability and limitations for practical applications. *Fluid Dynamics Research*, 45(3): 034501.
- Tang, G.H., Zhang, Y.H., Gu, X.J., and Emerson, D.R., 2008. Lattice Boltzmann modelling Knudsen layer effect in non-equilibrium flows. *Europhysics letters*, 83(4): 226–234.
- Tao, S., and Guo, Z.L., 2015. Boundary condition for lattice Boltzmann modeling of microscale gas flows with curved walls in the slip regime. *Physical Review E*, 91(4): 043305.
- Verhaeghe, F., Luo, L.S., and Blanpain, B., 2009. Lattice Boltzmann modeling of microchannel flow in slip flow regime. *Journal of Computational Physics*, 228(1): 147–157.
- Wang, S., Feng, Q.H., Javadpour, F., and Yang, Y.B., 2016. Breakdown of fast mass transport of methane through calcite nanopores. *The Journal of Physical Chemistry C*, 120(26): 10.
- Wang, X.K., and Sheng, J., 2017. Gas sorption and non-Darcy flow in shale reservoirs. *Petroleum Science*, 14(4): 746–754.
- Wang, Z.Y., Jin, X., Wang, X.Q., Sun, L., and Wang, M.R., 2016. Pore-scale geometry effects on gas permeability in shale. *Journal of Natural Gas Science and Engineering*, 34: 948–957.
- Wu, L., Ho, M.T., Germanou, L., Gu, X.J., Liu, C., Xu, K., and Zhang, Y.H., 2017. On the apparent permeability of porous media in rarefied gas flows. *Journal of Fluid Mechanics*, 822: 398–417.
- Xue, Q.Z., Tao, Y.H., Liu, Z.L., Lu, S.F., Li, X.F., Wu, T.T., Jin, Y.K., and Liu, X.F., 2015. Mechanism of oil molecules transportation in nano-sized shale channel: MD simulation. *RSC Advances*, 5(33): 25684–25692.
- Yu, H., Chen, J., Zhu, Y.B., Wang, F.C., and Wu, H.A., 2017. Multiscale transport mechanism of shale gas in micro/nanopores. *International Journal of Heat and Mass Transfer*, 111: 1172–1180.
- Zhai, G.Y., Wang, Y.F., Zhou, Z., Yu, S.F., Chen, X.L., and Zhang, Y.X., 2018. Exploration and research progress of shale gas in China. *China Geology*, 1: 257–272.
- Zhang, C.H., Chen, S.G., Sun, Q.C., and Jin, F., 2016. Free-surface simulations of Newtonian and non-Newtonian fluids with the lattice Boltzmann method. *Acta Geologica Sinica (English Edition)*, 90(3): 999–1010.
- Zhang, Raoyang, Shan, X.W., and Chen, H.D., 2006. Efficient kinetic method for fluid simulation beyond the Navier-Stokes equation. *Physical Review E*, 74(4): 046703.
- Zhang, T.Y., and Suen, C.Y., 1984. A fast parallel algorithm for thinning digital patterns. *Communications of the ACM*, 27(3): 236–239.
- Zhang, Y.H., Gu, X.J., Barber, R.W., and Emerson, D.R., 2006. Capturing Knudsen layer phenomena using a lattice Boltzmann model. *Physical Review E*, 74(4): 046704.
- Zhao, J.L., Yao, J., Li, A.F., Zhang, M., Zhang, L., Yang, Y.F., and Sun, H., 2016 a. Simulation of microscale gas flow in heterogeneous porous media based on the lattice Boltzmann method. *Journal of Applied Physics*, 120(8): 084306.
- Zhao, J.L., Yao, J., Zhang, L., Sui, H.G., and Zhang, M., 2016 b. Pore-scale simulation of shale gas production considering the adsorption effect. *International Journal of Heat and Mass Transfer*, 103: 1098–1107.
- Zheng, J.T., Wang, Z.Y., Gong, W.B., Ju, Y., and Wang, M.R., 2017. Characterization of nanopore morphology of shale and its effects on gas permeability. *Journal of Natural Gas Science and Engineering*, 47: 83–90.
- Zou, Q.S., and He, X.Y., 1997. On pressure and velocity boundary conditions for the lattice Boltzmann BGK model. *Physics of Fluids*, 9(6): 1591–1598.
- Zuo, H., Deng, S.C., and Li, H.B., 2019. Boundary scheme for lattice Boltzmann modeling of micro-scale gas flow in organic rich pores considering surface diffusion. *Chinese Physics B*, 28(3): 30202–030202.

About the first author



ZUO Hong, received his bachelor's degree from Huazhong University of Technology and Sciences, Wuhan, China, in 2016. In the same year, Zuo started his doctor's program in the University of Chinese Academy of Sciences, Beijing. Hong Zuo's doctor's program focuses on the multiscale flow.

About the corresponding author



DENG Shouchun, is a professor of Chinese Academy of Sciences, and awarded by the Hundred Talent Program of Chinese Academy of Sciences. He focuses on the economic exploitation of shale gas.